

Supplementary Information for:

Information-Rich High-Throughput Cellular Assays using Acoustic Mist Ionisation Mass Spectrometry

Martin Bachman,^{*a,b} Ian Sinclair,^b Delyan Ivanov,^c and Jonathan Wingfield^c

^a Discovery Science & Technology, Medicines Discovery Catapult, Alderley Park, UK. E-mail: martin.bachman@md.catapult.org.uk

^b Sample Management, Discovery Sciences, R&D, AstraZeneca, Alderley Park, UK.

^c Mechanistic Biology and Profiling, Discovery Sciences, R&D, AstraZeneca, Cambridge, UK.

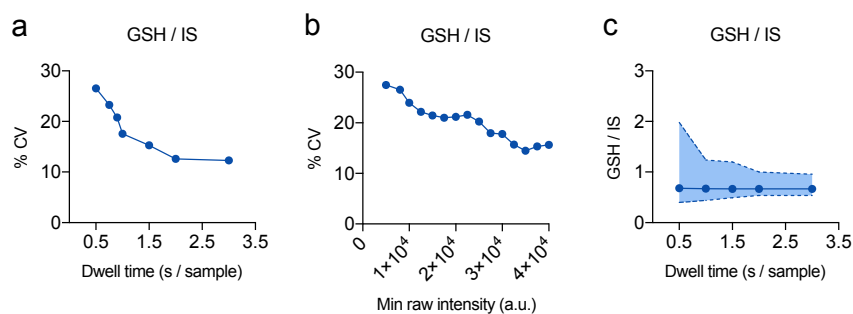


Fig. S1. Reproducibility of relative quantitation of glutathione (GSH) across a single 384-well plate (MCF7 cells) using GSH-¹³C₂,¹⁵N as an internal standard (IS) spiked into the lysis buffer. (a) Relationship between the coefficient of variation (CV) and sample throughput. (b) Relationship between the coefficient of variation and a minimum raw intensity threshold for individual 100 μ s MS scans (x axis). The threshold is calculated as the sum of GSH and IS signal intensities. (c) Relationship between the measurements of GSH (IS corrected) and sample throughput. Shown are average \pm range of measurements across a single 384-well plate.

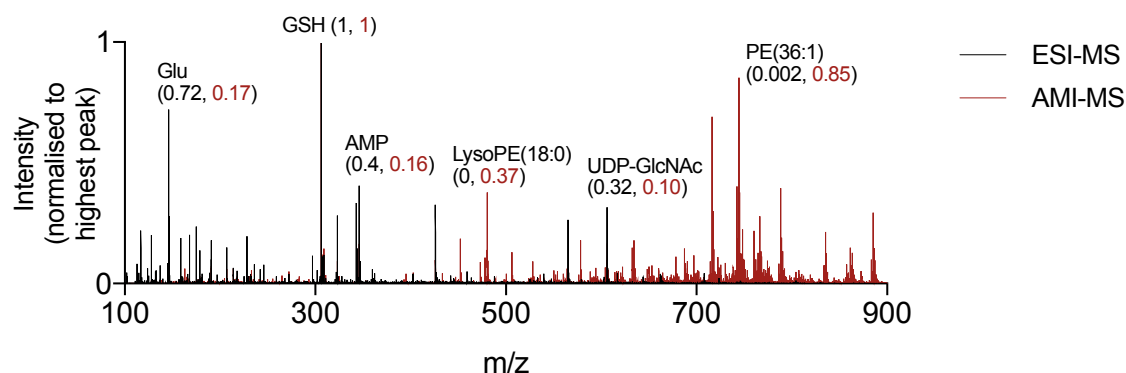


Fig. S2. Negative ion spectra of crude aqueous cell lysates (untreated caco-2 cells) acquired on AMI-MS and ESI-MS and normalized to the highest peak (glutathione at m/z 306.0765). AMI spectra are visibly richer in phospholipid species (650 – 900 Da), while ESI is more efficient for small polar species such as amino acids and nucleotides. Several species are highlighted, and their normalised intensities shown in brackets. Glu = glutamic acid, AMP = adenosine monophosphate, PE = phosphatidylethanolamine, UDP-GlcNAc = uridine diphosphate N-acetyl glucosamine.

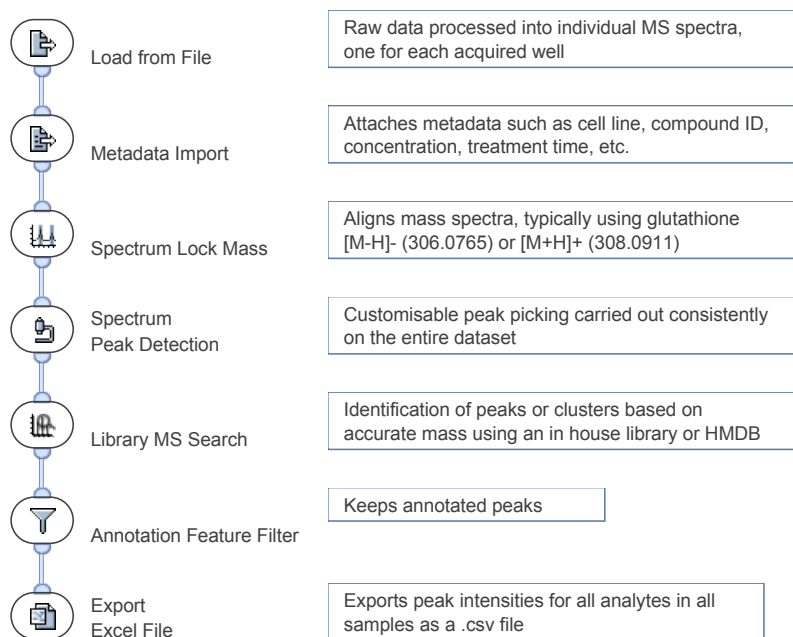


Fig. S3. Backbone of a typical data processing workflow in Genedata Expressionist. Many additional activities are available depending on the experimental design, biological questions or assay type.

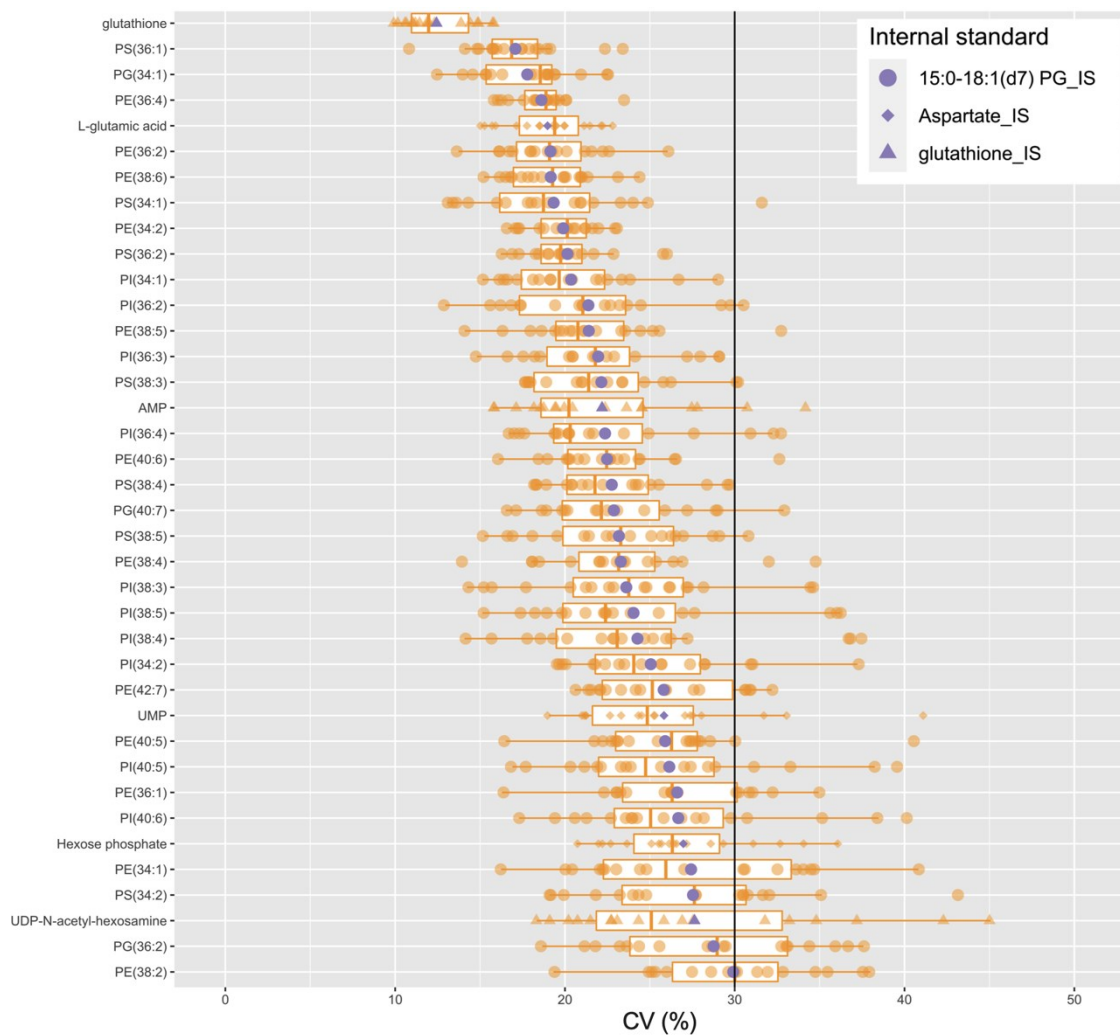


Fig. S4. Reproducibility of cellular assays with an AMI-MS end point. Untreated HepG2 cells were analysed across 7 independent experiments using a seeding density of 3500 cells per well and a 48 h incubation period. Shown are mean coefficient of variation (CV) (purple symbols, $n = 18$ plates) and CV from individual plates (orange symbols, $n = 352$ wells per plate). Underlaid box plots denote the median and interquartile range of individual plate CVs ($n = 18$). All analytes were normalised with an internal standard (see corresponding symbol shape on top right). AMP = adenosine monophosphate, UMP = uridine monophosphate, PE = phosphatidylethanolamine, PS = phosphatidylserine, PI = phosphatidylinositol, PG = phosphatidylglycerol.

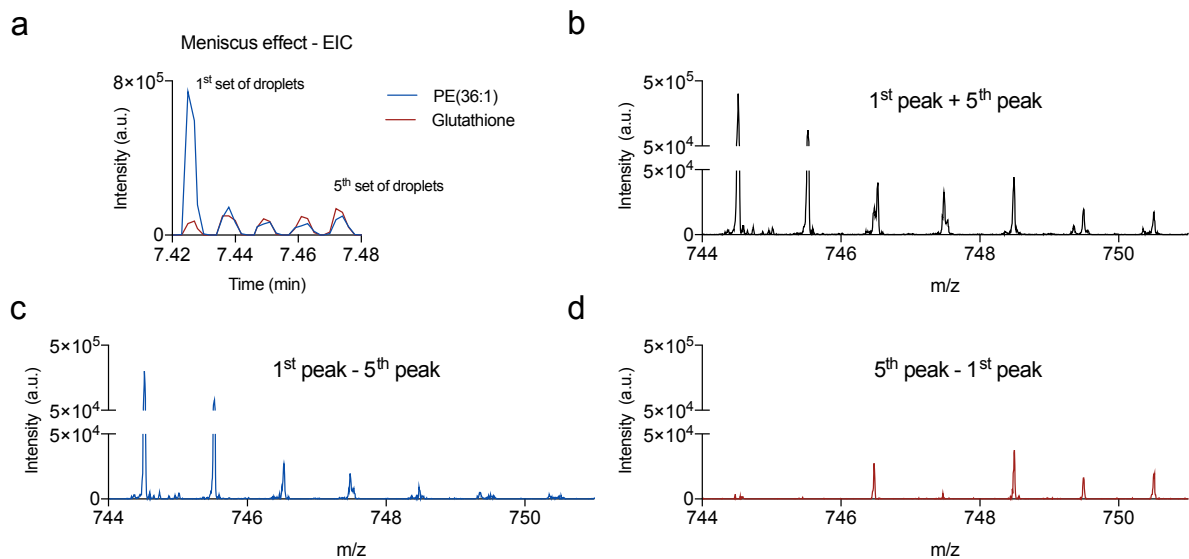


Figure S5. Natural enrichment of phospholipids at the surface of an aqueous lysate of human epithelial colorectal adenocarcinoma cells (10,000 Caco-2 cells per well). (a) Extracted ion chromatograms of an abundant phospholipid (PE(36:1)) and an abundant water-soluble metabolite (GSH) in 5 consecutive sets of misting events (20 nL each, total time 3.5 s). (b) Mass spectra combined from 1st and 5th peak. Natural isotopes of an abundant phospholipid PE(36:1) prevent relative quantitation of a lower abundant species (m/z 746.5). (c,d) Subtracted mass spectra (1st vs 5th peak) can reveal lower abundant species (e.g., 746.5 and 748.5 Da in (d)) and allow their relative quantitation.

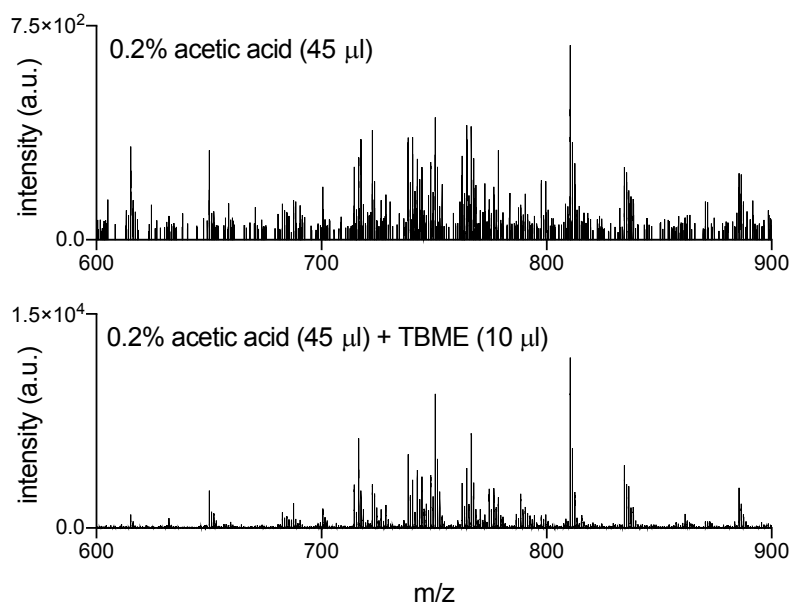


Figure S6. Addition of *tert*-butyl methyl ether (TBME) into an aqueous cell lysate further enriches phospholipids at the meniscus, resulting in an enhanced phospholipid region in AMI-MS spectra compared to aqueous lysate only. Spectra were acquired from an individual well containing 1000 hepatocytes (HepG2) before and after the addition of TBME.

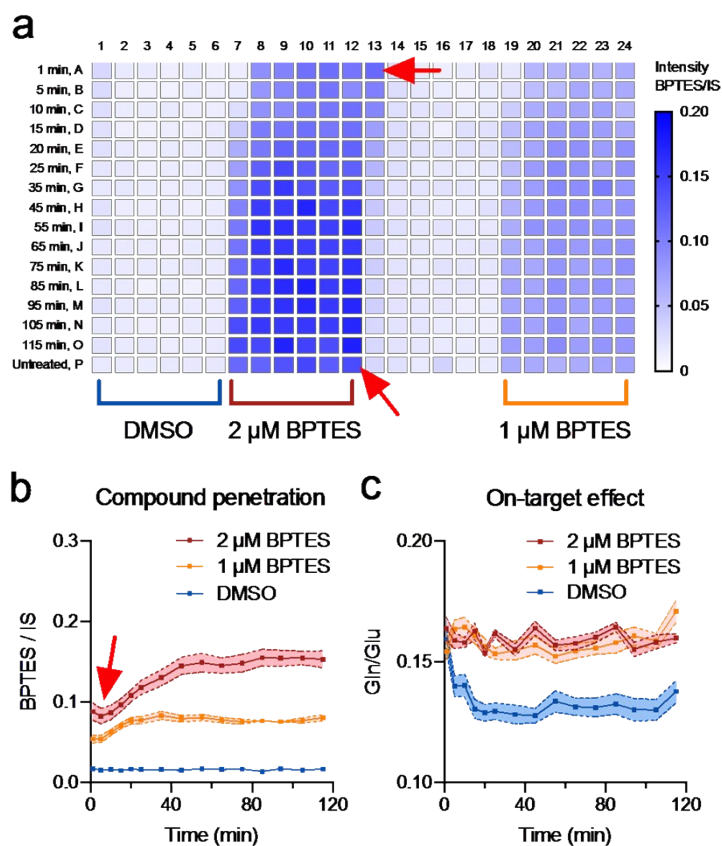


Fig. S7. Flow injection ESI-MS measurements of BPTES-treated caco-2 cells highlighting the carryover problems that can be encountered with chemically adsorbing compounds using contact-based in-solution MS methods. (a) Assay plate layout and a heatmap of BPTES intensity normalized to $^{13}\text{C}_2,^{15}\text{N}$ -glutathione internal standard (IS) across one dosed cell plate. Samples were injected in a column-wise discontinuous sequence (i.e., A1, B1, ..., P1, A2, B2, ..., P24), with acidified 60% organic mobile phase, 3 s pre-injection needle wash step using acidified acetonitrile, and a sample-to-sample run time of 45 s. Red arrows indicate clear carryover in untreated samples in samples P7-12, column 13, and also in early time points (e.g., wells A7-12). (b) BPTES penetration measurements are skewed as a result of this carryover (red and orange curves not originating close to 0). (c) Glutamine and glutamate (not chemically adsorbing) eluted cleanly within the first 12 s of sample run time and validated the AMI-MS measurements in Fig. 3c. Shown are mean \pm s.e.m. of 12 replicates for each condition and time point in (b) and (c).

Table S1. Selected commonly observed metabolites in AMI mass spectra of human cell lysates (here MCF7 cells) acquired in the negative ion mode. Shown are measured m/z values (deprotonated species only), signal-to-noise ratio (maximum intensity in a mass spectrum derived as a geometrical mean of all MS scans from 384 wells acquired in 3.4 min), and relative deviation from reference mass in parts per million (ppm). FA = fatty acid, PE = phosphatidylethanolamine, PS = phosphatidylserine, PI = phosphatidylinositol, PG = phosphatidylglycerol.

m/z (M-H)	ID	signal:noise	Error (ppm)	m/z (M-H)	ID	signal:noise	Error (ppm)
124.0069	Taurine	148.8	-4.1	506.3284	LysoPE(20:1)	9.9	6.4
127.0507	Pyroglutamine	12.5	-4.4	565.0521	UDP hexose	9.1	7.7
128.0350	Pyroglutamic acid	46.8	-2.3	571.2929	LysoPI(16:0)	9.5	7.0
131.0462	Asparagine	5.1	-0.1	579.0296	UDP-hexuronic acid	5.1	4.6
131.0822	Ornithine	5.4	-2.8	599.3216	LysoPI(18:0)	15.6	2.4
132.0295	Aspartic acid	5.7	-5.6	606.0784	UDP-N-acetyl-hexosamine	83.9	6.8
145.0614	Glutamine	206.9	-3.5	662.4812	PE(30:0)	13.9	7.0
146.0453	Glutamic acid	134.9	-4.3	688.4973	PE(32:1)	46.8	7.3
154.0614	Histidine	9.1	-5.1	690.5106	PE(32:0)	127.2	3.9
173.1037	Arginine	24.7	-3.8	714.5162	PE(34:2)	119	11.6
180.0655	Tyrosine	6.8	-6.0	716.5311	PE(34:1)	454.2	10.5
214.0476	Glycerophosphoethanolamine	251.8	-4.7	718.5409	PE(34:0)	130.6	2.3
218.1007	Pantothenic acid	5.8	-12.4	742.5465	PE(36:2)	409.1	9.8
255.2315	Palmitic acid	10.3	-5.8	744.5600	PE(36:1)	525.2	6.9
281.2480	Oleic acid	5.6	-2.0	747.5247	PG(34:1)	10.8	8.7
283.2642	Stearic acid	93.7	-0.2	760.5209	PS(34:1)	18.5	9.9
297.2432	FA(oxo-18:0)	22.6	-1.0	762.5336	PS(34:0)	45.4	5.9
299.2597	FA(hydroxy-18:0)	27.2	1.6	764.5306	PE(38:5)	76.6	9.2
306.0765	Glutathione, reduced	915.8	0.0	766.5405	PE(38:4)	68.9	1.7
323.0287	UMP	30.4	0.4	772.5952	PE(38:1)	19.5	11.7
346.0567	AMP	116.8	2.7	773.5417	PG(36:2)	20.1	10.2
362.0511	GMP	6.1	1.0	776.5648	PE(P-40:5)	8.9	6.2
402.9971	UDP	15.1	5.5	786.5340	PS(36:2)	5.9	6.2
426.0241	ADP	59.6	4.6	788.5492	PS(36:1)	60.2	5.7
442.0199	GDP	6.2	6.4	807.5132	PI(32:1)	13.3	12.7
450.2651	LysoPE(16:1)	58.8	5.5	809.5273	PI(32:0)	80.3	10.7
452.2804	LysoPE(16:0)	250.2	4.6	819.5249	PG(40:7)	13.9	8.2
465.3070	cholesterol sulfate	210	5.5	833.5290	PI(34:2)	10.6	12.5
478.2964	LysoPE(18:1)	192	5.2	835.5435	PI(34:1)	119.3	11.1
480.3123	LysoPE(18:0)	280.6	5.6	837.5582	PI(34:0)	87.4	9.9
500.2824	LysoPE(20:4)	13.1	8.3	861.5588	PI(36:2)	32.8	10.3
505.9918	ATP	10.4	6.5	863.5737	PI(36:1)	127.2	9.5